Research Square

Preprints are preliminary reports that have not undergone peer review.
They should not be considered conclusive, used to inform clinical practice,
or referenced by the media as validated information.

Markerless three-dimensional biomechanical analysis of manual flexible ureteroscopy: experience-related differences in wrist load during lower-calyx access

Satoshi Kobayashi

kobayashi.satoshi.282@m.kyushu-u.ac.jp

Kyushu University

Keiji Tsukino

Kyushu University

Mikifumi Koura

Kyushu University

Masaki Shiota

Kyushu University

Research Article

Keywords: flexible ureteroscopy, ergonomics, markerless motion capture, three-dimensional pose estimation, inverse dynamics, musculoskeletal disorders

Posted Date: November 20th, 2026

DOI: https://doi.org/10.21203/rs.3.rs-11136321/v1

License: This work is licensed under a Creative Commons Attribution 4.0 International License.
Read Full License

Additional Declarations: No competing interests reported.

Abstract

Purpose

To quantify upper-limb kinematics and estimated biomechanical load (a kinematics-derived load proxy, not measured muscle force) during simulated manual flexible ureteroscopy (fURS) using markerless 3D pose estimation, testing whether experience-related differences concentrate in lower-calyx access.

Methods

Eighteen urologists (10 experts, 8 novices) performed a phantom task: renal pelvis to upper, middle and lower calyx, returning to the pelvis between calyces. 3D landmarks from smartphone video (MediaPipe Pose) were converted to joint angles, jerk and inverse-dynamics load estimates. Primary outcomes were right-wrist force, jerk and angle in the lower-calyx phase; others were exploratory, analysed with participant-level Welch tests, Hedges g, 95% CIs, Holm correction and a mixed model for group × phase interaction.

Results

Procedure time was longer in novices (115.5 vs 61.5 s). In the lower-calyx phase, novices showed higher right-wrist force (1.87 vs 1.16 N; Holm $p = 0.026$), jerk (Holm $p = 0.020$) and angle (31.6° vs 24.9°; Holm $p = 0.026$), with no upper-calyx differences; force and jerk showed significant group × phase interactions ($p = 0.004$, 0.007) but angle did not ($p = 0.35$). Force, jerk and dispersion correlated strongly with movement speed ($\rho = 0.93–0.99$), and group differences were attenuated after speed adjustment.

Conclusion

In this simulator study, experience-related differences in estimated wrist load emerged mainly during lower-calyx access, whereas wrist angle differed throughout, pinpointing an ergonomic target. Because estimates were kinematics-derived and not EMG-validated, findings are hypothesis-generating; correlating them with physiological muscle activity is an important next step for robot-assisted ureteroscopy design.

Introduction

Flexible ureteroscopy (fURS) is central to minimally invasive stone and upper tract urothelial disease management; lower-pole access remains technically demanding due to infundibulopelvic anatomy and deflection required [1–3], and manual fURS imposes ergonomic strain linked to musculoskeletal symptoms, burnout and shortened careers [4–7].

Objective fURS ergonomic assessment is not new: surface electromyography (EMG) has described muscle activation during simulated fURS [8, 9], and motion tracking has defined ureteroscopic motion and kinematic efficiency, including an automated composite score [10, 11]. Our earlier study applied 2D markerless pose estimation to compare experts and novices by travel distance, speed, range and joint angle [12]. These approaches describe how the operator moves or which muscles activate, but none has estimated joint-level mechanical load from markerless video, and 2D analysis cannot resolve out-of-plane motion.

Sari et al. reported an approximately 9-fold higher risk of fURS failure for lower-pole stones larger than 17 mm [13], consistent with lower-calyx access being the most demanding part of the procedure; however, no study has directly tested this with detailed biomechanical data. The present study therefore extends prior work in three ways: tracking 3D landmarks of the arm, using a simplified physics-based model (inverse dynamics) that estimates joint-level load from these trajectories, and analysing this load by calyx phase. We hypothesised that right-wrist load differences would be larger during lower-calyx than upper-calyx access, and asked whether these load-based measures add information beyond the simpler kinematic measures — movement speed and path length — already used in prior work.

Materials and Methods

Participants and relationship to the earlier study

The study was approved by the Institutional Review Board of Kyushu University (approval no. 241321); all participants gave written informed consent. Of 19 right-handed urologists enrolled, one expert was excluded for left-hand scope use (a left–right confound), leaving 18: 10 experts (all male; Japanese Urological Association-certified, > 6 years' experience, > 50 fURS procedures) and 8 novices (6 male, 2 female; residents, 1–2 years' experience, < 5 procedures). The two female novices weighed under the model's 70-kg assumption (47, 53 kg), prompting a sensitivity analysis (see Statistical analysis). Sample size reflected participant availability, with no a priori calculation.

Twelve of the 18 participants (7 experts, 5 novices) also took part in our earlier 2D webcam-based study [12]; the smartphone footage recorded simultaneously in that study is reanalysed here in 3D, and the remaining 6 were newly recorded. For these 12, the present 3D path-length findings are therefore not independent of the earlier 2D findings, though all landmarks, force, jerk and phase-specific analyses here are newly derived — the earlier study reported only 2D travel distance, speed, range and joint angle, with no outcome overlap.

Phantom model and task

A kidney and bone phantom, 12/14 Fr access sheath and 8.4 Fr single-use flexible ureteroscope (285° deflection) were used as described previously [12]. Participants, facing the endoscopic monitor, advanced the scope to the renal pelvis, accessed the upper, middle and lower calyces in sequence,

returned to the pelvis between calyces, centred an artificial stone target on the monitor, and announced completion of each phase verbally.

Two investigators, aware of group allocation, independently marked phase boundaries (task start and arrival at each calyx) from these announcements; the upper-calyx phase ran from start to the upper calyx, and the middle and lower phases ran calyx-to-calyx (including withdrawal and re-entry), ending on arrival at the lower calyx.

Markerless 3D pose estimation and signal processing

Videos were recorded with a smartphone (iPhone 16 Pro; LiDAR-capable, though depth and calibration data were not captured or used) at 30 frames per second. 3D coordinates were extracted with MediaPipe Pose (v0.10.14, model complexity 2, confidence 0.5) using the model's world landmarks — metric coordinates in a hip-centred frame, with no external calibration or reference, so depth and scale are model estimates. Landmarks were the shoulders, elbows, wrists, index/pinky/thumb tips and hips, returned every frame, though occlusion accuracy is not guaranteed. To reduce small tracking jitter, coordinates were smoothed with a fourth-order zero-phase Butterworth low-pass filter (which removes frame-to-frame changes faster than 3 Hz) before calculating velocity and acceleration; this filter setting was fixed in advance rather than tuned to the data.

Estimated biomechanical load (inverse-dynamics model)

We estimated joint-level load with a simplified proximal-to-distal model using standard segment mass fractions (hand 0.6%, forearm 2.2%, upper arm 2.8%) [14] of a fixed 70-kg reference mass and fixed moment arms (wrist 0.015 m, elbow 0.040 m, shoulder 0.030 m; Supplementary Figure S1); segment lengths were per-trial median distances wrist–hand centroid (L_h), elbow–wrist (L_f) and shoulder–elbow (L_u). For each axis $i \in \{x, y, z\}$:

$$F_{wrist,i}(t) = L_h \cdot m_h \cdot a_{hand,i}(t) / r_{wrist}$$

$$F_{elbow,i}(t) = [L_f \cdot m_f \cdot a_{wrist,i}(t) + F_{wrist,i}(t) \cdot r_{wrist}] / r_{elbow}$$

$$F_{shoulder,i}(t) = [L_u \cdot m_u \cdot a_{elbow,i}(t) + F_{elbow,i}(t) \cdot r_{elbow}] / r_{shoulder}$$

where m is segment mass, a is acceleration of the hand centroid, wrist or elbow, and r is the moment arm; scalar load $F = (F_x^2 + F_y^2 + F_z^2)^{1/2}$. This simplified model accounts only for the force needed to accelerate each arm segment's mass; it excludes gravity, rotational effects and scope-handling force. Newton values are therefore nominal — proportional to assumed body mass — rather than muscle force measured by EMG or force sensors, and are termed *estimated biomechanical load*.

Outcome measures

Jerk — a standard measure of movement smoothness — was the magnitude of the third derivative of filtered joint position (m/s^3); higher values indicate less smooth, more erratic movement. Joint angles used 3D segment vectors: shoulder (trunk vs upper-arm), elbow (upper-arm vs forearm), wrist (forearm vs hand-centroid vector, 0° when collinear). Path length was cumulative 3D distance travelled by the filtered position (m), also expressed per second (mean speed). Force dispersion — the summed SD of F_x, F_y and F_z (N) — reflects how unstable the estimated force was over time; because this could simply track force size, we also computed a magnitude-independent alternative — mean resultant length of unit force vectors (0–1) — for directional consistency alone. Trunk sway (summed SD of mid-shoulder x/z, m) and shoulder tilt (mean absolute shoulder-line inclination, °) indexed whole-body postural compensation. A high-frequency (> 4 Hz) component, exploring possible hand tremor [15], cannot represent true tremor given the 3 Hz filter, and is reported only in Supplementary Table S1. Per participant and phase we used the frame-wise mean and 95th percentile (P95, a peak less sensitive to a single outlier frame than the true maximum).

Statistical analysis

The participant was the unit of analysis. Primary outcomes were right-wrist mean force, jerk and angle in the lower-calyx phase; all others were exploratory. Groups were compared with Welch's t-test (mean difference, 95% CI, Hedges g, Mann–Whitney p); the three primary p-values were Holm-adjusted. Exploratory outcomes were Holm-corrected both within each outcome across six anatomical sites and across all 90 whole-procedure comparisons (Supplementary Table S1); neither supports confirmatory claims. Phase dependence used a linear mixed-effects model (LMM; random intercept; group × phase; log-transformed where skewed). Robustness was checked by leave-one-out re-analysis and a frame-level LMM for the lower-calyx phase. Spearman's ρ and adjusted/unadjusted linear regression tested whether load variables add information beyond speed.

We rescaled the two female novices' force/dispersion to their actual weight (see Participants), analysing both possible assignments. Non-significant results are “no difference detected”, not equivalence. With 10 vs 8 participants, 80% power ($\alpha = 0.05$) applied only to $d \gtrsim 1.4$. Analyses used Python 3.11 (SciPy, statsmodels); code is publicly available (see Data availability).

Results

Participants and task duration

Experts (n = 10) and novices (n = 8) completed the task in 61.5 ± 14.9 s and 115.5 ± 55.5 s (difference 54.0 s, 95% CI 7.2–100.8; Mann–Whitney p = 0.007; Table 1); the lower-calyx phase showed the largest, most variable difference (24.3 ± 8.7 vs 55.5 ± 47.1 s), driven by two novices requiring 98 and 154 s.

Table 1
Task duration and right-wrist primary outcomes by calyx phase (participant-level)

Outcome (right wrist)	Phase	Experts	Novices	Difference (95% CI)	g	Welch p	Holm p*
Task duration (s)	Total	61.5 ± 14.9	115.5 ± 55.5	54.0 (7.2 to 100.8)	—	0.029	
	Upper	19.1 ± 7.2	31.6 ± 13.3	12.5 (0.9 to 24.1)	—	0.037	
	Middle	18.1 ± 8.1	28.4 ± 11.2	10.3 (0.0 to 20.5)	—	0.050	
	Lower	24.3 ± 8.7	55.5 ± 47.1	31.2 (-8.3 to 70.7)	—	0.105	
Force (N)	Upper	1.18 ± 0.40	1.21 ± 0.58	0.03 (-0.49 to 0.55)	0.06	0.906	
	Middle	1.09 ± 0.43	1.51 ± 0.82	0.41 (-0.30 to 1.13)	0.62	0.225	
	Lower	1.16 ± 0.39	1.87 ± 0.58	0.70 (0.18 to 1.23)	1.39	0.013	0.026
Jerk (m/s^3)	Upper	10.4 ± 3.6	11.7 ± 6.5	1.3 (-4.4 to 7.0)	0.23	0.636	
	Middle	9.5 ± 3.2	14.2 ± 8.1	4.7 (-2.2 to 11.7)	0.77	0.156	
	Lower	10.3 ± 3.5	17.7 ± 5.5	7.4 (2.5 to 12.4)	1.58	0.007	0.020
Wrist angle (°)	Upper	23.5 ± 4.6	28.7 ± 7.7	5.3 (-1.5 to 12.0)	0.82	0.116	
	Middle	24.3 ± 4.5	29.7 ± 6.0	5.4 (-0.1 to 10.9)	0.98	0.055	
	Lower	24.9 ± 4.8	31.6 ± 5.3	6.7 (1.6 to 11.9)	1.27	0.014	0.026

Values are mean ± SD (task duration in seconds; force, jerk and wrist-angle values are participant means). Difference = novice − expert (Welch 95% CI). g = Hedges g. *Holm-adjusted across the three primary outcomes (lower-calyx phase only); all other analyses, including task duration, are exploratory. Upper, middle and lower phases: start to arrival at the upper calyx; upper to middle; middle to lower (the last two include withdrawal to the pelvis). One expert was excluded from the 19 enrolled (left-hand scope holding). Participant-level values underlying this table are given in Supplementary Table S2.

Primary outcomes: right wrist during lower-calyx access

In the lower-calyx phase, novices showed higher right-wrist estimated force (1.87 vs 1.16 N; difference 0.70, 95% CI 0.18–1.23; g 1.39; Holm p = 0.026), jerk (17.7 vs 10.3 m/s^3; difference 7.4, 2.5–12.4; g 1.58;

Holm p = 0.020) and wrist angle (31.6 vs 24.9°; difference 6.7°, 1.6–11.9; g 1.27; Holm p = 0.026; Table 1, Fig. 1a; Supplementary Tables S3, S4); intervals are wide, and all three findings persisted on leave-one-out re-analysis (18/18 p < 0.05).

No difference was detected in the upper-calyx phase (Table 1). Group differences depended on phase for force (interaction p = 0.004; lower-calyx novice:expert ratio 1.62, 95% CI 1.14–2.28) and jerk (p = 0.007; ratio 1.73, 1.20–2.50), but not wrist angle (p = 0.35, higher in novices throughout). Median novice force rose across phases (1.06→1.28→1.75 N; Friedman p = 0.008), unlike experts (p = 0.067).

Rescaling to measured weights (47, 53 kg) reduced, but did not remove, the lower-calyx force difference (0.56–0.57 N; g 1.10; p = 0.039–0.041; Holm p ≈ 0.04); jerk and angle were unaffected by assumed mass.

Exploratory analyses

Across the whole procedure (90 exploratory comparisons, Supplementary Table S1), right-wrist path length was longer in novices (13.2 vs 4.8 m; g 1.81; p = 0.008) — the only result surviving Holm adjustment within its metric family — with novices also higher on right-elbow/shoulder force and time-normalized path length (Supplementary Table S1).

Force, jerk and force dispersion at the right wrist correlated almost perfectly with movement speed (Spearman ρ = 0.93, 0.99, 0.94; wrist angle ρ = 0.26; Table 2, Fig. 1b), and group differences in force and jerk were attenuated after speed adjustment (p = 0.68, 0.17), unlike wrist angle (p = 0.17). Force dispersion was higher in novices (p = 0.027) but tracked mean force (r = 0.95); adjusting for magnitude removed this difference, and directional consistency did not differ (Supplementary Table S1).

Table 2
Relationship of right-wrist load variables to movement speed

Right-wrist variable (whole procedure)	Spearman ρ with mean speed	Group difference, unadjusted	p	Group difference, speed-adjusted (95% CI)	p
Force	0.93	0.50	0.037	-0.06 (-0.35 to 0.23)	0.676
Jerk	0.99	5.7	0.015	-0.3 (-0.8 to 0.2)	0.169
Force dispersion	0.94	1.62	0.012	0.24 (-0.63 to 1.11)	0.562
Wrist angle	0.26	6.2	0.031	4.6 (-2.3 to 11.6)	0.174

Whole-procedure participant-level values (n = 18). Mean speed = path length/duration. Group differences are novice − expert from linear models with and without mean speed (unadjusted p from the same model, so it can differ slightly from the Welch p). Units: force N, jerk m/s^3, dispersion N, angle °.

Trunk sway and shoulder tilt showed no detectable difference, though intervals allow moderate-to-large effects (Supplementary Table S1). A frame-level sensitivity model for the lower-calyx phase (20,565

frames) gave right-wrist effects consistent with participant-level results, though these p-values likely understate uncertainty given frame autocorrelation and were not used for inference (Supplementary Table S3).

Discussion

We found right-wrist load — that is, estimated force — and jerk differences concentrated in the lower-calyx phase, while wrist angle was higher in novices throughout. These findings support the clinical view that lower-pole access is the most demanding part of the procedure [1–3], and reveal what whole-procedure averages had hidden: averaged overall, wrist findings were only borderline and participant-sensitive, whereas lower-calyx-specific findings held up consistently on leave-one-out re-analysis.

We also asked whether these newly estimated force and jerk values add anything that movement speed does not already show. Largely, they do not: force, jerk and force dispersion rose and fell with speed, and once we accounted for it, the expert-novice difference in force and jerk mostly disappeared — raising a fair question about whether the inverse-dynamics model's added complexity is worth it. Wrist angle, in contrast, remained only weakly related to speed and the group difference persisted after adjustment, perhaps making it the more valuable contribution of this approach. Prior work has documented EMG activation and movement efficiency in simulated fURS [8–11]; our data complement these, and the longer 3D path length in novices matches our prior 2D finding [12].

Our data do not support interpreting force dispersion as misdirected force: it was tightly coupled to force magnitude, and a magnitude-independent direction index showed no group difference (mean resultant length 0.014 vs 0.013; $p = 0.58$). The > 4 Hz component cannot represent physiological tremor, being indistinguishable from tracking noise; fatigue, tissue injury and patient outcomes were not assessed. Linking these estimates to fatigue, disease or patient safety would require EMG, symptom or clinical endpoints; they are candidate exposure measures only [16, 17].

Because this localized burden reflects manual wrist-manipulation mechanics, a fundamentally different operating mode — such as robotic assistance, with documented clinical efficacy and ergonomics [18–21] — may hold promise; our study cannot show robot-assisted ureteroscope reduces wrist load or angle.

Limitations. First, the simulator omitted real operating-room conditions such as a lead apron or assistants [22]. Second, the sample was small, unevenly split (10 vs 8), single-centre and unpowered a priori, detecting only large effects ($d \gtrsim 1.4$); non-significant findings do not imply no difference. One expert was excluded for protocol deviation, 12 of 18 participants overlap with our earlier study, and this one-off design cannot address long-term outcomes. Third, experience was confounded with age and body size (see Participants and Results), and the load model's simplifications (see Estimated biomechanical load) remain unvalidated against EMG or motion capture [23]. Fourth, the smartphone-based pipeline's depth/occlusion error is unquantified [24], wrist angle only approximates orientation, and true tremor cannot be analysed [25]. Phase boundaries, marked independently by two unblinded

investigators from verbal announcements, showed excellent inter-rater agreement (ICC(2,1) ≥ 0.998, mean absolute difference ≤ 0.7 s; Supplementary Table S5), and re-deriving durations from the second investigator's timestamps gave unchanged results (middle/lower phases include pelvis withdrawal).

Conclusion

This simulator study introduces a markerless, AI-based 3D approach to estimating biomechanical load on a surgeon's upper limb during fURS — the first, to our knowledge, for flexible ureteroscopy amid a rapidly growing field of markerless ergonomic risk assessment elsewhere [27]. Right-wrist load and jerk differences were largest during lower-calyx access, while wrist angle was higher in novices throughout, pinpointing where ergonomic burden concentrates; sex and body-size differences between groups remain a potential confound, and these kinematics-derived, EMG-unvalidated estimates are hypothesis-generating.

Abbreviations

3D, three-dimensional;

CI, confidence interval;

fURS, flexible ureteroscopy;

EMG, electromyography;

LMM, linear mixed-effects model.

Declarations

Competing interests:

The authors declare no financial competing interests. The authors declare no non-financial competing interests.

Ethics approval:

The study was approved by the Institutional Review Board of Kyushu University (approval no. 241321). All procedures were performed in accordance with the ethical standards of the institutional research committee and with the 1964 Helsinki Declaration and its later amendments. No animals were used.

Informed consent:

Written informed consent was obtained from all participants, who were given clear opportunities to opt out.

Funding:

This study was supported by JSPS KAKENHI (grant numbers JP23K19219 and 25K15937), the Japanese Foundation for Research and Promotion of Endoscopy Grant, the Cancer Support Association Grant (2025), and the Japanese Society of Endourology and Robotics Robot-Assisted Surgery Research Grant A (2024).

Author Contribution

SK: protocol/project development, data collection and management, data analysis, and manuscript writing/editing. KT: project development, data collection, and data analysis. MK: data collection and manuscript writing/editing. MS: protocol/project development (supervision), manuscript writing/editing. All authors read and approved the final version.

Acknowledgement

This study was supported by JSPS KAKENHI (grant numbers JP23K19219 and 25K15937), the Japanese Foundation for Research and Promotion of Endoscopy Grant, the Cancer Support Association Grant (2025), and the Japanese Society of Endourology and Robotics Robot-Assisted Surgery Research Grant A (2024).

Data Availability

Data availability: Analysis code is publicly available at https://doi.org/10.5281/zenodo.22908546. The data that support this study's findings are available from the corresponding author upon reasonable request.

References

1. Wiseman O, Smith D, Starr K et al (2025) The PUrE randomized controlled trial 1: Clinical and cost effectiveness of flexible ureterorenoscopy and extracorporeal shockwave lithotripsy for lower pole stones of ≤ 10 mm. Eur Urol 88:179–189. https://doi.org/10.1016/j.eururo.2025.02.002
2. Dresner SL, Iremashvili V, Best SL, Hedican SP, Nakada SY (2020) Influence of Lower Pole Infundibulopelvic Angle on Success of Retrograde Flexible Ureteroscopy and Laser Lithotripsy for the Treatment of Renal Stones. J Endourol 34:655–660. https://doi.org/10.1089/end.2019.0720
3. Jacquemet B, Martin L, Pastori J et al (2014) Comparison of the efficacy and morbidity of flexible ureterorenoscopy for lower pole stones compared with other renal locations. J Endourol 28:1183–1187. https://doi.org/10.1089/end.2014.0286

4. Ong CSH, Castellani D, Gorelov D et al (2022) Role and Importance of Ergonomics in Retrograde Intrarenal Surgery: Outcomes of a Narrative Review. J Endourol 36:1–12. https://doi.org/10.1089/end.2021.0326
5. Gabrielson AT, Tanidir Y, Castellani D et al (2022) A Global Survey of Ergonomics Practice Patterns and Rates of Musculoskeletal Pain Among Urologists Performing Retrograde Intrarenal Surgery. J Endourol 36:1168–1176. https://doi.org/10.1089/end.2022.0075
6. Epstein S, Sparer EH, Tran BN et al (2018) Prevalence of Work-Related Musculoskeletal Disorders Among Surgeons and Interventionalists: A Systematic Review and Meta-analysis. JAMA Surg 153:e174947. https://doi.org/10.1001/jamasurg.2017.4947
7. Tjiam IM, Goossens RH, Schout BM et al (2014) Ergonomics in endourology and laparoscopy: an overview of musculoskeletal problems in urology. J Endourol 28:605–611. https://doi.org/10.1089/end.2013.0654
8. Wright HC, Gheordunescu G, O'Laughlin K et al (2022) Ergonomics in the OR: An Electromyographic Evaluation of Common Muscle Groups Used During Simulated Flexible Ureteroscopy - a Pilot Study. Urology 170:66–72. https://doi.org/10.1016/j.urology.2022.08.028
9. Ludwig WW, Lee G, Ziemba JB, Ko JS, Matlaga BR (2017) Evaluating the Ergonomics of Flexible Ureteroscopy. J Endourol 31:1062–1066. https://doi.org/10.1089/end.2017.0378
10. Valovska MT, Gomez G, Fineman R et al (2022) Analysis of Flexible Ureteroscopic Motion and Kinematic Efficiency: A Simulation-Based Pilot Study. J Endourol 36:855–861. https://doi.org/10.1089/end.2021.0726
11. Valovska MT, Yang J, Chen N, Yu D, Wollin DA (2023) Development of an Automated Composite Ureteroscopic Efficiency Score Through Simulated Ureteroscopic Skills Assessment. J Endourol 37:956–964. https://doi.org/10.1089/end.2022.0820
12. Kobayashi S, Tsukino K, Koura M et al (2026) Quantifying ergonomic challenges for urologists operating flexible ureteroscopes through artificial intelligence-based posture estimation. World J Urol 44:347. https://doi.org/10.1007/s00345-026-06444-8
13. Sari S, Ozok HU, Topaloglu H, Cakici MC, Ozdemir H, Karakoyunlu AN, Senturk AB, Ersoy H (2017) The association of a number of anatomical factors with the success of retrograde intrarenal surgery in lower calyceal stones. Urol J 14:4008–4014. https://doi.org/10.22037/uj.v14i4.4034
14. Riemer R, Hsiao-Wecksler ET (2009) Improving net joint torque calculations through a two-step optimization method for estimating body segment parameters. J Biomech Eng 131:011007. https://doi.org/10.1115/1.3005155
15. Kuliś S, Callegari B, Maszczyk A, Pietraszewski P (2025) Physiological limb tremor modulation by physical exertion: a systematic review and meta-analysis in healthy adults. Br Med Bull 156:ldaf022. https://doi.org/10.1093/bmb/ldaf022
16. Merbah J, Caré BR, Gorce P, Gadea F, Prince F (2023) A New Approach to Quantifying Muscular Fatigue Using Wearable EMG Sensors during Surgery: An Ergonomic Case Study. Sens (Basel) 23:1686. https://doi.org/10.3390/s23031686

17. Reijmerink IM, van der Laan MJ, Wietasch JKG, Hooft L, Cnossen F (2024) Impact of fatigue in surgeons on performance and patient outcome: systematic review. Br J Surg 111:znad397. https://doi.org/10.1093/bjs/znad397
18. Gopi P, Ishfaq M, Shkoukani ZW et al (2025) Robotic Flexible Ureteroscopy: Systematic Review and Meta-Analysis of Surgical Efficacy, Safety and Ergonomic Outcomes. Cureus 17:e90447. https://doi.org/10.7759/cureus.90447
19. Ergül RB, Özervarli MF, Panthier F et al (2025) Surgical outcomes of robotic surgery for kidney stones: a systematic review and meta-analysis from section of YAU and EAU endourology. World J Urol 43:364. https://doi.org/10.1007/s00345-025-05734-x
20. El-Hajj A, Abou Chawareb E, Zein M, Wahoud N (2024) First prospective clinical assessment of the ILY® robotic flexible ureteroscopy platform. World J Urol 42:143. https://doi.org/10.1007/s00345-024-04869-7
21. Kim J, Park H, Kwon DS, Lee JY, Cho SY (2025) Robotic flexible ureteroscopy system, Zamenix R, demonstrates efficacy and safety in initial clinical evaluation for retrograde intrarenal surgery. Sci Rep 15:17366. https://doi.org/10.1038/s41598-025-94031-z
22. Gardner AK, Kaji AH, Boermeester M (2024) Practical Guide to Surgical Simulation Research. JAMA Surg 159:453–454. https://doi.org/10.1001/jamasurg.2023.6684
23. Wen J, Raison M, Achiche S (2018) Using a cost function based on kinematics and electromyographic data to quantify muscle forces. J Biomech 80:151–158. https://doi.org/10.1016/j.jbiomech.2018.09.002
24. Rode D, Dunkel A, Willi R, Wolf P, Xiloyannis M, Riener R (2025) Assessment of monocular human pose estimation models for clinical movement analysis. Sci Rep 15:38767. https://doi.org/10.1038/s41598-025-22626-7
25. Agostinelli T, Generosi A, Ceccacci S, Mengoni M (2024) Validation of computer vision-based ergonomic risk assessment tools for real manufacturing environments. Sci Rep 14:27785. https://doi.org/10.1038/s41598-024-79373-4
26. Van Nortwick SS, Lendvay TS, Jensen AR, Wright AS, Horvath KD, Kim S (2010) Methodologies for establishing validity in surgical simulation studies. Surgery 147:622–630. https://doi.org/10.1016/j.surg.2009.10.068
27. Scataglini S, Fontinovo E, Khafaga N, Khan MU, Khan MF, Truijen S (2025) A systematic review of the accuracy, validity, and reliability of markerless versus marker camera-based 3D motion capture for industrial ergonomic risk analysis. Sens (Basel) 25:5513. https://doi.org/10.3390/s25175513

Figures

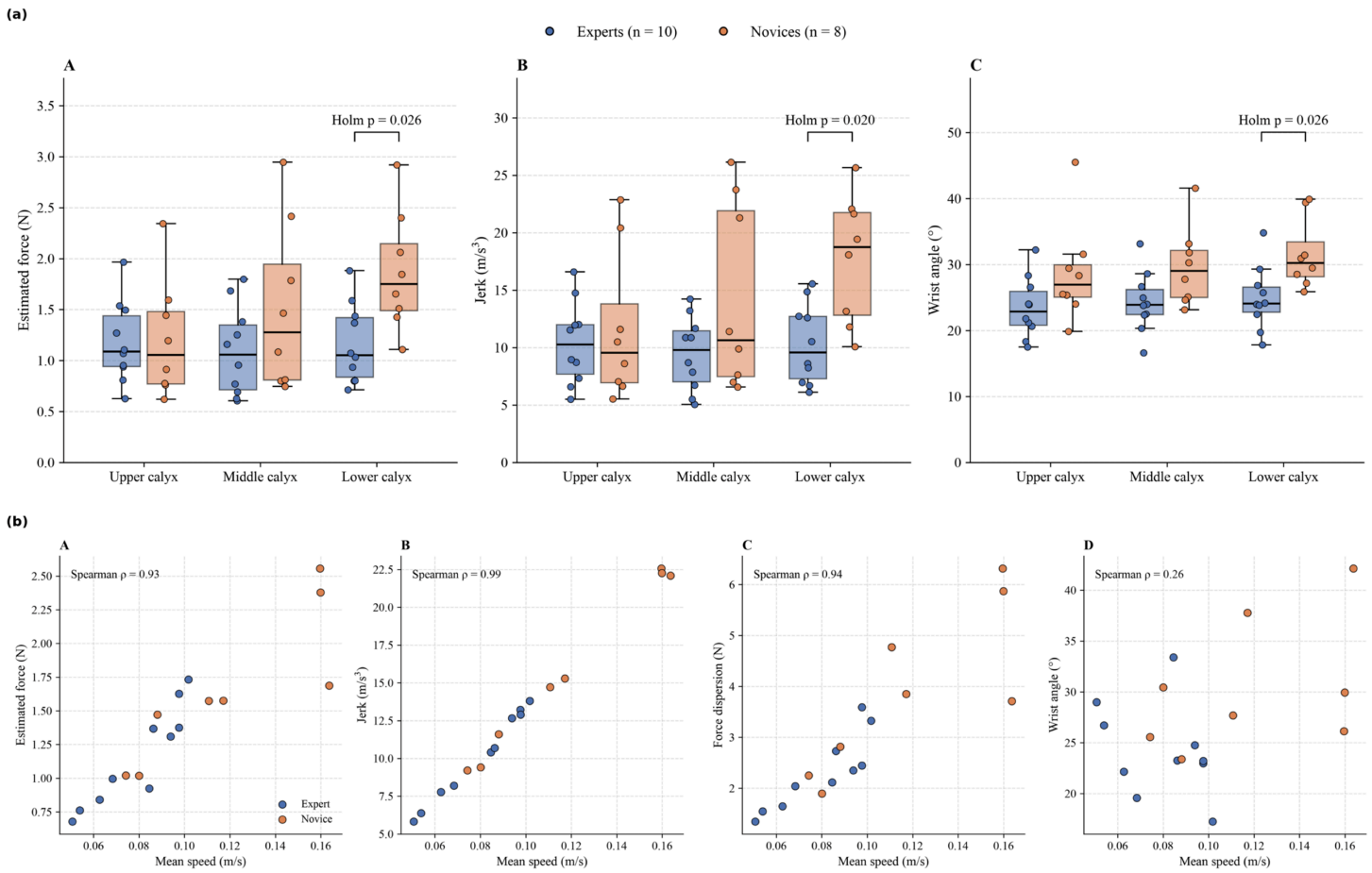


Figure 1. Right-wrist ergonomic outcomes

a. Estimated force, jerk and wrist angle at the right wrist during the upper-, middle- and lower-calyx phases of the phantom task. Box plots show the distribution for each phase, with individual participants overlaid (experts, n = 10, blue circles; novices, n = 8, orange circles). Novices showed higher force and jerk than experts only during lower-calyx access, while wrist angle was higher in novices throughout all three phases, indicating that wrist posture, rather than force or jerk, was a persistent feature of novice performance across the procedure. Force is a nominal value from a simplified inertial model, proportional to assumed body mass, and does not represent measured muscle force.

b. Relationship between estimated load and movement speed. Scatter plots show right-wrist force, jerk, force dispersion and wrist angle plotted against each participant's mean movement speed (path length divided by task duration; n = 18; experts, blue circles; novices, orange circles). Force, jerk and force dispersion rose and fell together with movement speed almost in lockstep, whereas wrist angle varied largely independently of speed, suggesting that wrist angle captures information about technique that speed alone does not.

Figure 1

See image above for figure legend.

Supplementary Files

This is a list of supplementary files associated with this preprint. Click to download.

- SupplementaryFigureS1SatoshiKobayashi.tiff
- SupplementaryTablesSatoshiKobayashi.docx